Journal of Computational Physics 229 (2010) 2034–2045

Contents lists available at ScienceDirect

Journal of Computational Physics

journal homepage: www.elsevier.com/locate/jcp

A numerical scheme for the Green–Naghdi model

O. Le Métayer *, S. Gavrilyuk, S. Hank

Aix-Marseille Université, IUSTI, UMR CNRS 6595, Technopôle de Château Gombert, 5 Rue E. Fermi, 13453 Marseille Cedex 13, France
INRIA SMASH Project, 2004 route des Lucioles, 06902 Sophia Antipolis, France

ARTICLE INFO

Article history:
Received 6 April 2009
Received in revised form 9 November 2009
Accepted 10 November 2009
Available online 16 December 2009

Keywords:
Dispersive waves
Green–Naghdi model
Solitary waves
Godunov type method

ABSTRACT

In this paper a hybrid numerical method using a Godunov type scheme is proposed to solve the Green–Naghdi model describing dispersive "shallow water" waves. The corresponding equations are rewritten in terms of new variables adapted for numerical studies. In particular, the numerical scheme preserves the dynamics of solitary waves. Some numerical results are shown and compared to exact and/or experimental ones in different and significant configurations. A dam-break problem and an impact problem where a liquid cylinder is falling to a rigid wall are solved numerically. This last configuration is also compared with experiments leading to a good qualitative agreement.

1. Introduction

Much work has been done in the derivation of relatively simple mathematical models of long non-linear water waves. One of popular models is the Green–Naghdi model obtained in the one-dimensional case by Su and Gardner [19] and in the multi-dimensional case by Green et al. [10,11] within the context of a homogeneous one-layer fluid. In the literature, this model is usually called Green–Naghdi model (GN model or GN system). A derivation of the GN model based on the variational formulation of the Euler equations was done by Miles and Salmon [15] (see also [17,18]). A mathematical justification of the GN model was done by Makarenko [14] and Alvarez-Samaniego and Lannes [1]. Camassa et al. [5] proposed a Hamiltonian formulation of the GN model. Nadiga et al. [16] made a comparison between the full Euler equations and the GN model. They have, in particular, shown that the GN model predicts important features of the flow (excluding wave breaking) accurately over a wide range of parameters. Solitary wave solutions of the GN model were obtained by Su and Gardner [19]. The linear stability of solitary waves was recently proved by Li [13]. A criterium of stability of shear flows for the GN model was proposed by Gavrilyuk and Teshukov [9]. A wide class of multi-dimensional solutions and approximate solutions of non-linear multi-dimensional GN model has been found by Gavrilyuk and Teshukov [8] and Teshukov and Gavrilyuk [20]. Unsteady undular bores were described by El et al. [6].

The aim of this article is to give a numerical algorithm of the Godunov type for the GN model preserving, in particular, solitary wave solutions. This problem was also addressed in Yan and Shu [23] and Bernetti et al. [4] for the KdV equation. Recently, Antuono et al. [2] and Grosso et al. [12] have proposed an original approach based on a hyperbolic approximation of dispersive equations. This approach is very attractive even if the corresponding hyperbolic system contains stiff source terms and admits resonances (the case where some eigenvalues can coincide at singular hypersurfaces).

* Corresponding author. Address: Aix-Marseille Université, IUSTI, UMR CNRS 6595, Technopôle de Château Gombert, 5 Rue E. Fermi, 13453 Marseille Cedex 13, France.
E-mail addresses: olivier.lemetayer@polytech.univ-mrs.fr (O. Le Métayer), sergey.gavrilyuk@polytech.univ-mrs.fr (S. Gavrilyuk), sarah.hank@polytech.univ-mrs.fr (S. Hank).

0021-9991/$ - see front matter © 2009 Elsevier Inc. All rights reserved.
doi:10.1016/j.jcp.2009.11.021

The structure of the article is organized as follows. In Section 2 the Green–Naghdi model is presented. In Sections 3 and 4 a change of variables is made and the governing equations are rewritten with these new variables. The numerical method is derived in Section 5 and is tested in Section 6 on solitary waves solutions of the GN model. In this last section new results on the dam-break problem and the impact of a falling cylinder on a rigid surface are also presented.

2. The Green–Naghdi model

Consider the Green–Naghdi equations describing dispersive non-linear long water waves in a single layer over a flat bottom $z = 0$. The dissipation effects are neglected. Under these assumptions the Green–Naghdi equations read [5,8,10,11,15,17–19]:

$$\begin{aligned} &\frac{\partial h}{\partial t} + div(h\mathbf{u}) = 0 \\ &\frac{\partial h\mathbf{u}}{\partial t} + div(h\mathbf{u}\otimes\mathbf{u} + pI) = 0, \quad p = \frac{gh^2}{2} + \frac{1}{3}h^2\ddot{h} \end{aligned} \tag{1}$$

Here $h > 0$ is the total water depth and $\mathbf{u}$ is the average horizontal velocity. The "dot" means the material derivative:

$$\dot{h} = \frac{\partial h}{\partial t} + \mathbf{u}\cdot\nabla\mathbf{h}$$

The pressure can also be written in the form:

$$p \equiv h\left(\frac{\partial W}{\partial h} - \frac{\partial}{\partial t}\left(\frac{\partial W}{\partial \dot{h}}\right) - div\left(\frac{\partial W}{\partial \dot{h}}\mathbf{u}\right)\right) - W = h\frac{\delta W}{\delta h} - W,$$

where the potential W is:

$$W(h,\dot{h}) = \frac{gh^2}{2} - \frac{h\dot{h}^2}{6}$$

The system (1) admits the variational formulation with the Lagrangian

$$\mathcal{L} = \int_{\Omega_t}\left(\frac{h|\mathbf{u}|^2}{2} - W(h,\dot{h})\right)d\Omega = \int_{\Omega_t} L d\Omega, \quad L = \frac{h|\mathbf{u}|^2}{2} - W(h,\dot{h})$$

where Ω_t is a two-dimensional domain occupied by the fluid [18]. The mass conservation law should be considered as a constraint for such a variational formulation.

We define the energy in the form

$$E(h,\tau) = W(h,\dot{h}) + \dot{h}\tau, \quad \tau = -\frac{\partial W}{\partial \dot{h}} = \frac{1}{3}h\dot{h}$$

Obviously

$$\frac{\partial E(h,\tau)}{\partial h} = \frac{\partial W}{\partial h}, \quad \frac{\partial E(h,\tau)}{\partial \tau} = \dot{h}$$

For the GN system the energy is:

$$E(h,\tau) = \frac{gh^2}{2} + \frac{h\dot{h}^2}{6} = \frac{gh^2}{2} + \frac{3}{2}\frac{\tau^2}{h}$$

The equation of the energy is then:

$$\frac{\partial}{\partial t}\left(\frac{h|\mathbf{u}|^2}{2} + E\right) + div\left(\mathbf{u}\left(\frac{h|\mathbf{u}|^2}{2} + E + p\right)\right) = 0 \tag{2}$$

When dispersive terms in (1) and (2) are neglected, the conventional hyperbolic shallow water equations are recovered.

3. Change of variables

The aim of this paragraph is to present an equivalent formulation of the GN model by using a new set of unknowns instead of conventional unknowns $(h,\mathbf{u})$. The idea of this change of variables (which is not local) comes from the definition of potential flows of the GN system [5,15,17,18]. It can be shown that the conventional definition where the potential φ is defined by the formula $\mathbf{u} = \nabla\varphi$ is not a solution of the GN model because the corresponding compatibility conditions are not satisfied (in the multi-dimensional case). It was found in Gavrilyuk and Gouin [7] that the true definition of "potential flows"

for a general class of Lagrangians can be done in the following way. Let us rewrite the Lagrangian density as a function of h and $\mathbf{j} = h\mathbf{u}$, and define the variable:

$$\mathbf{K} = \frac{\delta L}{\delta \mathbf{j}} = \frac{\partial L}{\partial \mathbf{j}}$$

For the GN model

$$L = \frac{|\mathbf{j}|^2}{2h} - W\left(h, \frac{\partial h}{\partial t} + \frac{\mathbf{j}\cdot\nabla h}{h}\right) = \frac{|\mathbf{j}|^2}{2h} - \frac{gh^2}{2} + \frac{h}{6}\left(\frac{\partial h}{\partial t} + \frac{\mathbf{j}\cdot\nabla h}{h}\right)^2$$

Hence

$$\mathbf{K} = \frac{\partial L}{\partial \mathbf{j}} = \mathbf{u} + \frac{\dot{h}}{3}\nabla h$$

The flow is potential if there exists a scalar function φ such that $\mathbf{K} = \nabla\varphi$.

It can be shown that with such a definition, a generalized Bernoulli integral exists (see, for example, [8]). The following equivalence relation can be formulated: $\mathbf{K}_1 \sim \mathbf{K}_2$ if there exists ψ such that $\mathbf{K}_1 - \mathbf{K}_2 = \nabla\psi$. In particular, an equivalent definition of potential flows can be:

$$\mathbf{K} = \mathbf{u} + \frac{1}{3h}\nabla\left(h^2\dot{h}\right) \tag{3}$$

Indeed,

$$\mathbf{u} + \frac{1}{3h}\nabla\left(h^2\dot{h}\right) = \mathbf{u} + \frac{2\dot{h}}{3}\nabla h + \frac{h}{3}\nabla\dot{h} = \mathbf{u} + \frac{\dot{h}}{3}\nabla h + \frac{\dot{h}}{3}\nabla h + \frac{h}{3}\nabla\dot{h} = \mathbf{u} + \frac{\dot{h}}{3}\nabla h + \frac{1}{3}\nabla\left(h\dot{h}\right)$$

As in [5,15,17,18], we adopt definition (3). We will rewrite the GN model in terms of $(h, \mathbf{K})$ variables rather than in $(h, \mathbf{u})$ variables. It follows from (1) and (3) that

$$\frac{\partial h\mathbf{K}}{\partial t} + div\left(h\mathbf{u}\otimes\mathbf{K} - \frac{1}{3}\mathbf{u}\otimes\nabla\left(h^2\dot{h}\right) + \left(\frac{gh^2}{2} + \frac{1}{3}h^2\ddot{h} - \frac{1}{3}\left(h^2\dot{h}\right)_t\right)I\right) = 0$$

or in equivalent form,

$$\frac{\partial h\mathbf{K}}{\partial t} + div\left(h\mathbf{u}\otimes\mathbf{K} - \frac{1}{3}\mathbf{u}\otimes\nabla\left(h^2\dot{h}\right) + \frac{1}{3}\mathbf{u}\cdot\nabla\left(h^2\dot{h}\right)I + \left(\frac{gh^2}{2} + \frac{1}{3}h^2\ddot{h} - \frac{1}{3}\left(h^2\dot{h}\right)_t - \frac{1}{3}\mathbf{u}\cdot\nabla\left(h^2\dot{h}\right)\right)I\right) = 0$$

Here we have adopted the definition that the divergence of a second order tensor is a covector whose components are the divergence of each columns. With this definition

$$div(\mathbf{a}\otimes\mathbf{b}) = \mathbf{b}div(\mathbf{a}) + \frac{\partial\mathbf{b}}{\partial\mathbf{x}}\mathbf{a}$$

Since

$$\frac{1}{3}h^2\ddot{h} - \frac{1}{3}\left(h^2\dot{h}\right)_t - \frac{1}{3}\mathbf{u}\cdot\nabla\left(h^2\dot{h}\right) = -\frac{2}{3}h\dot{h}^2$$

we finally get

$$\frac{\partial h}{\partial t} + div(h\mathbf{u}) = 0 \tag{4}$$

$$\frac{\partial h\mathbf{K}}{\partial t} + div\left(h\mathbf{u}\otimes\mathbf{K} - \frac{1}{3}\mathbf{u}\otimes\nabla\left(h^2\dot{h}\right) + \left(\frac{gh^2}{2} - \frac{2}{3}h\dot{h}^2 + \frac{1}{3}\mathbf{u}\cdot\nabla\left(h^2\dot{h}\right)\right)I\right) = 0 \tag{5}$$

Another equivalent form of the momentum Eq. (5) is:

$$\frac{\partial h\mathbf{K}}{\partial t} + div\left(h\mathbf{K}\otimes\mathbf{u} - \frac{1}{3}\nabla\left(h^2\dot{h}\right)\otimes\mathbf{u} + \left(\frac{gh^2}{2} - \frac{2}{3}h\dot{h}^2 + \frac{1}{3}\mathbf{u}\cdot\nabla\left(h^2\dot{h}\right)\right)I\right) = 0 \tag{6}$$

The advantage of the presentations (5) and (6) is that the fluxes do not contain the second time derivatives of h.

Nevertheless an additional treatment when dealing with the numerical method is necessary to retrieve $\mathbf{u}$ from $\mathbf{K}$. Indeed if $h\mathbf{K}$ is known, the variable $h\mathbf{u}$ is defined from the following elliptic equation

$$h\mathbf{K} = h\mathbf{u} - \frac{1}{3}\nabla\left(h^3 div\mathbf{u}\right) \tag{7}$$

where either the Neumann condition $\frac{\partial \mathbf{u}}{\partial \mathbf{n}} = 0$ or periodic ones are considered at the boundary of a calculation domain. The idea to replace the variable $\mathbf{u}$ by $\mathbf{K}$ was firstly used in [5] for Hamiltonian formulation of the GN model. Then this elliptic equation which can also be taken under the following form:

$$h\mathbf{K} = h\mathbf{u} - \frac{1}{3}\nabla\left(h^2 div(h\mathbf{u})\right) + \frac{1}{6}\nabla\left(h\mathbf{u}\cdot\nabla\left(h^2\right)\right) \tag{8}$$

has to be solved numerically. It is worth to note that in such a presentation only h^2 and $h\mathbf{u}$ should be estimated, other powers of h do not appear here. This presentation (8) will be used for the construction of the numerical procedure.

4. One-dimensional configuration: plane and cylindrical geometry

In this section the governing equations in a form adapted for the study of plane and cylindrical waves are presented. Let (r,θ), $\mathbf{e}_r = (\cos\theta, \sin\theta)^T$ and $\mathbf{e}_\theta = (-\sin\theta, \cos\theta)^T$ be the polar coordinates and the corresponding orthonormal curvilinear basis respectively. Obviously,

$$\frac{\partial \mathbf{e}_r}{\partial r} = 0, \quad \frac{\partial \mathbf{e}_r}{\partial \theta} = \mathbf{e}_\theta, \quad \nabla\theta = \frac{\mathbf{e}_\theta}{r}, \quad \frac{\partial \mathbf{e}_r}{\partial \mathbf{x}} = \frac{\partial \mathbf{e}_r}{\partial r}\otimes\nabla r + \frac{\partial \mathbf{e}_r}{\partial \theta}\otimes\nabla\theta = \mathbf{e}_\theta\otimes\nabla\theta = \frac{\mathbf{e}_\theta\otimes\mathbf{e}_\theta}{r}$$

Hence

$$div(\mathbf{e}_r\otimes\mathbf{e}_r) = \mathbf{e}_r div(\mathbf{e}_r) + \frac{\partial \mathbf{e}_r}{\partial \mathbf{x}}\mathbf{e}_r = \mathbf{e}_r div(\mathbf{e}_r) + \frac{(\mathbf{e}_\theta\otimes\mathbf{e}_\theta)\mathbf{e}_r}{r} = \mathbf{e}_r div(\mathbf{e}_r) = \frac{\mathbf{e}_r}{r}$$

and for any scalar f

$$div(f(\mathbf{e}_r\otimes\mathbf{e}_r)) = \frac{f\mathbf{e}_r}{r} + \mathbf{e}_r(\nabla f\cdot\mathbf{e}_r) = \frac{f\mathbf{e}_r}{r} + \mathbf{e}_r(\nabla f\cdot\mathbf{e}_r) = \mathbf{e}_r\left(\frac{\partial f}{\partial r} + \frac{f}{r}\right) = \frac{\mathbf{e}_r}{r}\frac{\partial (rf)}{\partial r}$$

Then for the case where all the variables depend only on (t,r) we have

$$\mathbf{K} = K\mathbf{e}_r, \quad \mathbf{u} = u\mathbf{e}_r$$

$$div(h\mathbf{u}) = \frac{1}{r}\frac{\partial (ru)}{\partial r}, \quad \nabla f = \frac{\partial f}{\partial r}\mathbf{e}_r$$

$$\begin{aligned} &div\left(h\mathbf{K}\otimes\mathbf{u} - \frac{1}{3}\nabla\left(h^2\dot{h}\right)\otimes\mathbf{u} + \left(\frac{gh^2}{2} - \frac{2}{3}h\dot{h}^2 + \frac{1}{3}\mathbf{u}\cdot\nabla\left(h^2\dot{h}\right)\right)I\right) \\ &= div\left(\left(hKu - \frac{1}{3}u\frac{\partial\left(h^2\dot{h}\right)}{\partial r}\right)\mathbf{e}_r\otimes\mathbf{e}_r + \left(\frac{gh^2}{2} - \frac{2}{3}h\dot{h}^2 + \frac{1}{3}u\frac{\partial\left(h^2\dot{h}\right)}{\partial r}\right)I\right) \\ &= \left(\frac{1}{r}\frac{\partial}{\partial r}\left(r\left(hKu - \frac{1}{3}u\frac{\partial\left(h^2\dot{h}\right)}{\partial r}\right)\right) + \frac{\partial}{\partial r}\left(\frac{gh^2}{2} - \frac{2}{3}h\dot{h}^2 + \frac{1}{3}u\frac{\partial\left(h^2\dot{h}\right)}{\partial r}\right)\right)\mathbf{e}_r \end{aligned}$$

Hence, the GN equations in polar coordinates are

$$\begin{aligned} &\frac{\partial h}{\partial t} + \frac{1}{r}\frac{\partial (rhu)}{\partial r} = 0 \\ &\frac{\partial hK}{\partial t} + \frac{\partial (hKu)}{\partial r} + \frac{\partial}{\partial r}\left(\frac{gh^2}{2} - \frac{2}{3}h^3\left(\frac{\partial u}{\partial r} + \frac{u}{r}\right)^2\right) = -\frac{hu^2}{r} \\ &hK = hu - \frac{1}{3}\frac{\partial}{\partial r}\left(h^2\left(\frac{\partial (hu)}{\partial r} + \frac{hu}{r}\right)\right) + \frac{1}{6}\frac{\partial}{\partial r}\left(hu\frac{\partial (h^2)}{\partial r}\right) \end{aligned}$$

Universal expressions for both types of geometry (plane or radial symmetry) are:

$$\begin{aligned} &\frac{\partial h}{\partial t} + \frac{1}{r^\nu}\frac{\partial (r^\nu hu)}{\partial r} = 0 \\ &\frac{\partial hK}{\partial t} + \frac{\partial}{\partial r}\left(hKu + \frac{gh^2}{2} - \frac{2}{3}h^3\left(\frac{\partial u}{\partial r} + \frac{\nu u}{r}\right)^2\right) = -\frac{\nu hu^2}{r} \\ &hK = hu - \frac{1}{3}\frac{\partial}{\partial r}\left(h^2\left(\frac{\partial hu}{\partial r} + \frac{\nu hu}{r}\right)\right) + \frac{1}{6}\frac{\partial}{\partial r}\left(hu\frac{\partial h^2}{\partial r}\right) \end{aligned} \tag{9}$$

Here $\nu = 1$ is for cylindrical geometry, and $\nu = 0$ is for plane geometry. In the latter case the variable r will be replaced by x.

5. Numerical scheme

For the sake of clarity let us consider the plane geometry ($v = 0$ and r is replaced by x in (9)):

$$\begin{cases} \frac{\partial h}{\partial t} + \frac{\partial (hu)}{\partial x} = 0 \\ \frac{\partial hK}{\partial t} + \frac{\partial \left(hKu + \frac{gh^2}{2} + \alpha \right)}{\partial x} = 0 \end{cases} \tag{10}$$

where

$$K = u - \frac{1}{3h} \frac{\partial}{\partial x} \left(h^3 \frac{\partial u}{\partial x} \right) \tag{11}$$

$$\alpha = -\frac{2}{3} h^3 \left(\frac{\partial u}{\partial x} \right)^2 \tag{12}$$

The preceding system (10) can be written in conservative form:

$$\frac{\partial \mathbf{U}}{\partial t} + \frac{\partial \mathbf{F}}{\partial x} = 0 \tag{13}$$

where

$$\mathbf{U} = \begin{pmatrix} h \\ hK \end{pmatrix}, \quad \mathbf{F} = \begin{pmatrix} hu \\ hKu + \frac{gh^2}{2} + \alpha \end{pmatrix}$$

The numerical resolution of this system involves some difficulties. The first one is related to the presence of dispersive effects and associated discretized terms. The second one is related to the determination of the velocity u when the conservative variables h and hK are known. In the following, all these difficulties are treated using an explicit algorithm based on a Godunov type scheme and the resolution of an ordinary differential equation. But a significant care must be taken when dealing with dispersive effects. Consequently, the conventional numerical procedure needs important extensions that are detailed hereafter. The numerical resolution of system (10) is then divided in three successive steps:

- the numerical approximations of the terms containing spatial derivatives (K and α from relations (11) and (12) respectively),
- the time evolution of the conservative variables h and hK using a Godunov type scheme,
- the resolution of an ordinary differential equation to obtain the values of velocity u from variables h and hK.

Let us consider a numerical cell defined as $C_i = [x_{i-1/2}, x_{i+1/2}]$ (the center of the cell is located at x_i and the spatial increment is denoted by $\Delta x = x_{i+1/2} - x_{i-1/2}$). The time increment is defined as $\Delta t = t^{n+1} - t^n$.

Integrating in space and time the system (10) the associated numerical scheme is obtained:

$$\mathbf{U}_i^{n+1} = \mathbf{U}_i^n - \frac{\Delta t}{\Delta x} \left(\mathbf{F}_{i+1/2}^* - \mathbf{F}_{i-1/2}^* \right) \tag{14}$$

where $\mathbf{U}_i^{n+1}$ and $\mathbf{U}_i^n$ are constant states inside the numerical cell C_i at times t^{n+1} and t^n respectively. The variables $\mathbf{F}_{i+1/2}^*$ and $\mathbf{F}_{i-1/2}^*$ are the constant fluxes across interfaces between cells during the time step.

Usually these fluxes are determined by solving the Riemann problem associated to the system under study. When the system is hyperbolic an exact solution of the Riemann problem may be obtained. In this case the fluxes are computed exactly and the numerical system (14) corresponds to the Godunov scheme. However, the system (10) is dispersive, an exact solution of the Riemann problem is no longer available. In this case an approximate Riemann solver must be used to compute these fluxes.

Concerning our applications the most appropriate is the *HLL* Riemann solver. Indeed this solver guarantees the conservation of variables linked to the equations of system (13), that is conservation of mass and momentum. In addition only two waves are taken into account in this solver corresponding to those associated to the shallow water equations (system (10)) without dispersive terms. Moreover this solver provides simple explicit formulas for fluxes as explained hereafter.

At each interface between numerical cells, the flux vector $\mathbf{F}^*$ is needed. Let us denote by subscripts L and R the states on both sides of the discontinuity and by superscript *HLL* the corresponding solution of the solver. Then the following relations holds:

$$\begin{cases} \mathbf{F}_L - \sigma_L \mathbf{U}_L = \mathbf{F}^{HLL} - \sigma_L \mathbf{U}^{HLL} \\ \mathbf{F}_R - \sigma_R \mathbf{U}_R = \mathbf{F}^{HLL} - \sigma_R \mathbf{U}^{HLL} \end{cases} \tag{15}$$

Combining equations of system (15), the flux solution is directly obtained by:

$$\mathbf{F}^{HLL} = \frac{\sigma_R \mathbf{F}_L - \sigma_L \mathbf{F}_R - \sigma_R \sigma_L (\mathbf{U}_L - \mathbf{U}_R)}{\sigma_R - \sigma_L} \tag{16}$$

In these equations, σ_L and σ_R are estimates of the wave speeds associated to the shallow water system, that is $u \pm \sqrt{gh}$. The last assumption is based on the following fact. The phase velocity of linear dispersive waves for the GN model linearized on a constant state $h_0 > 0$ with zero velocity $u = 0$, is always smaller than the velocity of long waves. Indeed, the phase velocity c_p of progressive waves is

$$c_p^2 = \frac{gh_0}{1 + h_0 k/3} < gh_0$$

where k is the wave number. Then this estimation is correct at least for waves of small amplitude.

By using relation (16) fluxes of system (14) write:

$$\begin{cases} \mathbf{F}^*_{i+1/2} = \mathbf{F}^{HLL}_{i+1/2} = \frac{\sigma_{R,i+1/2}\mathbf{F}^n_i - \sigma_{L,i+1/2}\mathbf{F}^n_{i+1} - \sigma_{R,i+1/2}\sigma_{L,i+1/2}\left(\mathbf{U}^n_i - \mathbf{U}^n_{i+1}\right)}{\sigma_{R,i+1/2} - \sigma_{L,i+1/2}} \\ \mathbf{F}^*_{i-1/2} = \mathbf{F}^{HLL}_{i-1/2} = \frac{\sigma_{R,i-1/2}\mathbf{F}^n_{i-1} - \sigma_{L,i-1/2}\mathbf{F}^n_i - \sigma_{R,i-1/2}\sigma_{L,i-1/2}\left(\mathbf{U}^n_{i-1} - \mathbf{U}^n_i\right)}{\sigma_{R,i-1/2} - \sigma_{L,i-1/2}} \end{cases} \tag{17}$$

Since the initial states $\mathbf{U}^n_i$ and $\mathbf{F}^n_i$ are known the flux solutions are fully determined by relations (17) as well as the conservative variables h and hK at time t^{n+1} by the Godunov type scheme (14).

Now concerning the determination of the states $\mathbf{U}^n_i$ and the associated fluxes $\mathbf{F}^n_i$, conventional finite difference discretizations are considered for spatial derivatives. From system (13), only the terms K and α contain such derivatives and rewrite (see also (7)):

$$K = u - \frac{h}{3}\frac{\partial^2(hu)}{\partial x^2} + \frac{u}{6}\frac{\partial^2 h^2}{\partial x^2} - \frac{1}{6h}\frac{\partial h^2}{\partial x}\frac{\partial(hu)}{\partial x} \tag{18}$$

$$\alpha = -\frac{2}{3h}\left(h\frac{\partial(hu)}{\partial x} - \frac{u}{2}\frac{\partial h^2}{\partial x}\right)^2 \tag{19}$$

The numerical estimation of the first and second order derivatives of any variable β (here $\beta = h^2$ or $\beta = hu$) are given by the following relations:

$$\begin{cases} \left(\frac{\partial\beta}{\partial x}\right)_i = \frac{\beta_{i+1} - \beta_{i-1}}{2\Delta x} \\ \left(\frac{\partial^2\beta}{\partial x^2}\right)_i = \frac{\beta_{i+1} + \beta_{i-1} - 2\beta_i}{(\Delta x)^2} \end{cases} \tag{20}$$

When using these discretizations at time t^n, the states $\mathbf{U}^n_i$ and fluxes $\mathbf{F}^n_i$ are now fully determined.

The last ingredient concerns the determination of the velocity u_i at time t^{n+1} when the conservative variables h^{n+1}_i and $(hK)^{n+1}_i$ are known. For this, Eq. (18) is considered. It can be written in the following form:

$$\frac{\partial^2(hu)}{\partial x^2} + \frac{1}{2h^2}\frac{\partial h^2}{\partial x}\frac{\partial(hu)}{\partial x} - \frac{1}{2h^2}\left(6 + \frac{\partial^2 h^2}{\partial x^2}\right)(hu) + \frac{3}{h^2}(hK) = 0 \tag{21}$$

or

$$\frac{\partial^2(hu)}{\partial x^2} + A\frac{\partial(hu)}{\partial x} + B(hu) + C = 0 \tag{22}$$

where

$$A = \frac{1}{2h^2}\frac{\partial h^2}{\partial x}$$

$$B = -\frac{1}{2h^2}\left(6 + \frac{\partial^2 h^2}{\partial x^2}\right)$$

$$C = \frac{3}{h^2}(hK)$$

The discretized version of Eq. (22) writes:

$$\left(\frac{\partial^2(hu)}{\partial x^2}\right)_i + A_i\left(\frac{\partial(hu)}{\partial x}\right)_i + B_i(hu)_i + C_i = 0 \tag{23}$$

with

$$\left(\frac{\partial^2(hu)}{\partial x^2}\right)_i = \frac{(hu)_{i+1} + (hu)_{i-1} - 2(hu)_i}{(\Delta x)^2}$$

$$\left(\frac{\partial(hu)}{\partial x}\right)_i = \frac{(hu)_{i+1} - (hu)_{i-1}}{2\Delta x}$$

$$A_i = \frac{1}{2h_i^2}\frac{h_{i+1}^2 - h_{i-1}^2}{2\Delta x}$$
$$B_i = -\frac{1}{2h_i^2}\left(6 + \frac{h_{i+1}^2 + h_{i-1}^2 - 2h_i^2}{(\Delta x)^2}\right)$$
$$C_i = \frac{3}{h_i^2}(hK)_i$$

All the variables in the preceding relation are those at time t^{n+1}. As a consequence, the variables $h_i,\ h_i^2$ and $(hK)_i$ are known and come from the time evolution of conservative variables with the help of the Godunov type scheme presented above. The only unknowns are the terms $(hu)_i$ in each numerical cell. Relation (23) applied in each cell represents a system that can be solved either by a direct (Gauss) or an iterative (Jacobi, Gauss–Seidel) method. Once this system is solved, the velocity u_i is determined in all the domain. Computational problems may arise in the limit $h_i \to 0$. To avoid this singularity in case of problems involving wet/dry bed interface, we added at the dry bed an artificial thin layer whose presence did not influence the flow characteristics (see also discussion of such a problem in [3]).

The next section is devoted to numerical results obtained with the present method in different configurations.

6. Numerical results

6.1. Comparison with exact solutions

6.1.1. "Shallow water" equations

When dispersive effects are neglected the Green–Naghdi system (10) reads:

$$\begin{cases} \frac{\partial h}{\partial t} + \frac{\partial (hu)}{\partial x} = 0 \\ \frac{\partial hu}{\partial t} + \frac{\partial \left(hu^2 + \frac{gh^2}{2}\right)}{\partial x} = 0 \end{cases} \tag{24}$$

The system (24) without dispersive terms is recovered when $K = u$ and $\alpha = 0$ in system (10) and corresponds to the "shallow water" equations.

The numerical method proposed in this paper in order to solve the Green–Naghdi model is now used to compute the following Riemann problem associated to "shallow water" equations:

$$\left.\begin{pmatrix} h \\ u \end{pmatrix}\right|_{t=0} = \begin{cases} \begin{pmatrix} h^- = 1.8\ \text{m} \\ u^- = 0 \end{pmatrix}, & \text{if } x < 300\ \text{m} \\ \begin{pmatrix} h^+ = 1\ \text{m} \\ u^+ = 0 \end{pmatrix}, & \text{if } x > 300\ \text{m} \end{cases} \tag{25}$$

The explicit solution of the Riemann problem is simple and can be found, for example, in [21,22].

For completeness, we present it below.

In the domain $-\infty < x/t < -\sqrt{gh^-}$ the solution is constant: $u = 0,\ h = h^-$.

In the domain $-\sqrt{gh^-} < x/t < u^* - \sqrt{gh^*}$ the solution is a rarefaction fan determined by relations $u + 2\sqrt{gh} = 2\sqrt{gh^-},\ x/t = u - \sqrt{gh}$.

In the domain $u^* - \sqrt{gh^*} < x/t < \sigma$ the solution is constant $u = u^*,\ h = h^*$.

Finally, the solution is constant in the domain $\sigma < x/t < \infty$: $u = u^+,\ h = h^+$.

Here $h^*,\ u^*$ and the velocity of the hydraulic jump σ are determined through the following algebraic relations representing the continuity of the left Riemann invariant $u + 2\sqrt{gh}$ and the Rankine–Hugoniot relations at the hydraulic jump:

$$u^* + 2\sqrt{gh^*} = 2\sqrt{gh^-}, \quad h^*(u^* - \sigma) = -h^+\sigma, \quad h^*(u^* - \sigma)^2 + g(h^*)^2/2 = h^+\sigma^2 + g(h^+)^2/2$$

The numerical results have been obtained by using 1000 numerical cells, the Courant number is 0.8. The numerical (symbols) and exact (lines) solutions associated to the previous Riemann problem are presented in Fig. 1 at time $t = 57$ s. Both results are in total agreement.

6.1.2. Solitary wave solutions

We are looking for solitary waves for the Green–Naghdi system of equations $(h(\xi), u(\xi))$, where $\xi = x - \mathcal{D}t$ and $\mathcal{D}$ is a constant:

$$\begin{cases} h_t + (hu)_x = 0 \\ (hu)_t + (hu^2 + p)_x = 0 \end{cases}$$

where the pressure p is here given by:

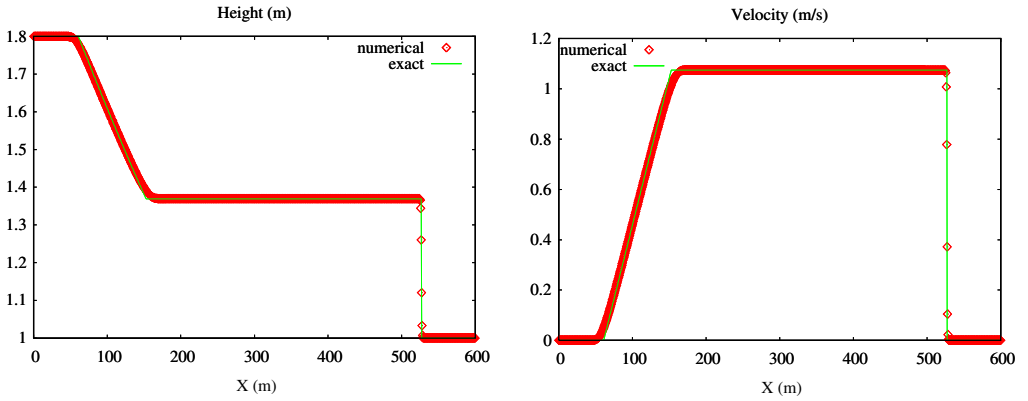

Fig. 1. Exact (lines) and numerical (symbols) solutions of the Riemann problem (25).

$$p = \frac{1}{2}gh^2 + \frac{1}{3}h^2\ddot{h}$$

Integration gives us [19]:

$$h(\xi) = h_1 + (h_2 - h_1)\mathrm{sech}^2\left(\frac{\xi}{2}\sqrt{\frac{3(h_2 - h_1)}{h_2 h_1^2}}\right)$$

$$u(\xi) = \mathcal{D}\left(1 - \frac{h_1}{h(\xi)}\right)$$

where h_1 is the layer depth at infinity and h_2 corresponds to the crest of a solitary wave. The soliton velocity $\mathcal{D}$ is related to h_2 by the following formula:

$$\mathcal{D}^2 = gh_2$$

In the following example, $h_1 = 10$ m, $h_2 = 12.1$ m and $g = 10$ m s^{-2} leading to $\mathcal{D} = 11$ m/s.

The numerical results (with 1000 cells) are shown in dotted lines in Fig. 2 at different successive times: $t = 0$, $t = 7.3$ s, $t = 14.6$ s, $t = 21.9$ s and $t = 29.2$ s.

The Neumann boundary conditions have been used and the Courant number is 0.8. Three thousand time steps have been considered to achieve this simulation.

The last result is compared to the exact solution (lines). Again both results are in excellent agreement showing the capability of the present method to reproduce the dynamics of solitary waves.

In the following test case, periodic boundary conditions have been used in order to appreciate the propagation of a solitary wave at long time. The initial data of the soliton are: $h_1 = 10$ m, $h_2 = 22.5$ m, $g = 10$ m s^{-2} leading to $\mathcal{D} = 15$ m/s.

The numerical results (with 5000 cells) are represented in Fig. 3 at 10 different successive times corresponding to 5 loops over the domain. The number of time steps is 25,000 that corresponds to 80 s of the total time of simulation. It can be clearly seen that the wave amplitudes as well as their shapes are perfectly conserved during the calculation.

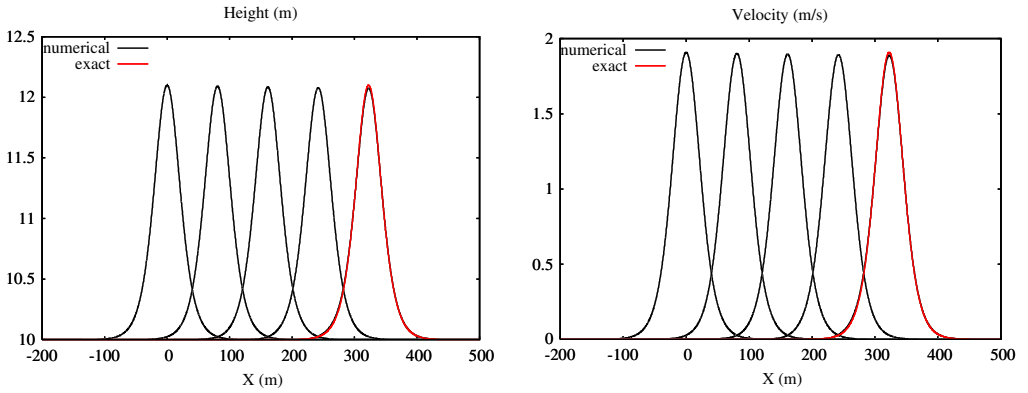

Fig. 2. Numerical solutions (dotted curves) at different times representing the propagation of a solitary wave. The exact solution (continuous curve) is also represented at the final time.

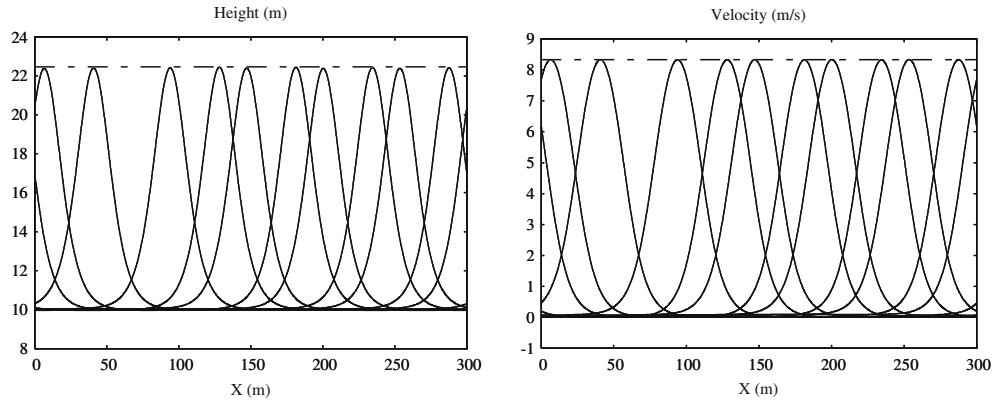

Fig. 3. Numerical solutions (continuous curves) at 10 different time instants (8 s,16 s, . . . , 80 s) representing the propagation of a solitary wave after 5 loops over the domain with periodic boundary conditions. The wave amplitudes as well as their shapes do not change in time.

A convergence test has been made to study the accuracy of the method as well as the influence of the numerical resolution for different numbers of numerical cells: 100, 1000 and 10,000.

The relative error based on the L^2-norm, represented in Fig. 4 as a function of time for each mesh size, shows the convergence of the numerical method. The relative norm is in the form

$$||h - h_{ref}||_{L_2} / ||h_{ref} - h_1||_{L_2}$$

where h_{ref} is the exact solitary wave solution, and h_1 is the value of the free surface at infinity.

6.2. Dam-break problem for the GN system

A dam-break problem for the Green–Naghdi model (1) is now considered with the initial data (25) previously proposed in the 'Shallow water equations' section:

$$\left.\begin{pmatrix} h \\ u \end{pmatrix}\right|_{t=0} = \begin{cases} \begin{pmatrix} h^- = 1.8\ \text{m} \\ u^- = 0 \end{pmatrix}, & \text{if } x < 0\ \text{m} \\ \begin{pmatrix} h^+ = 1\ \text{m} \\ u^+ = 0 \end{pmatrix}, & \text{if } x > 0\ \text{m} \end{cases} \tag{26}$$

The structure of the resulting solution is quite complicated since the governing equations do not admit self-similar solutions (see [6] for discussion of the solution of the Riemann problem and relation to the modulation equations for the GN model).

Let us remark that, in general, discontinuous initial data of this type are not well adapted if a finite difference scheme is used to solve this problem. Our numerical method is also able to deal with discontinuous initial data even if dispersive effects are taken into account.

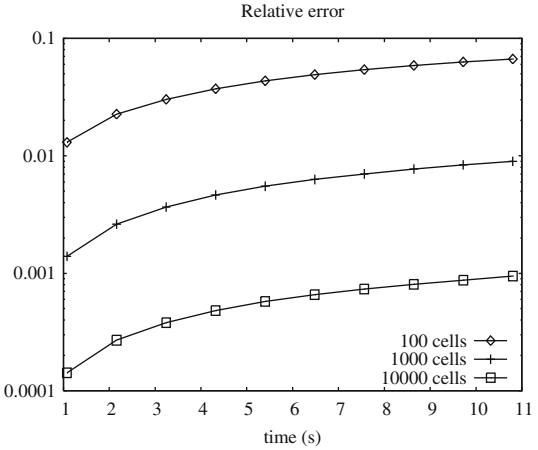

Fig. 4. Relative errors (in logarithmic scale) based on the L^2-norm as function of time for three different mesh sizes: 100, 1000 and 10,000 numerical cells.

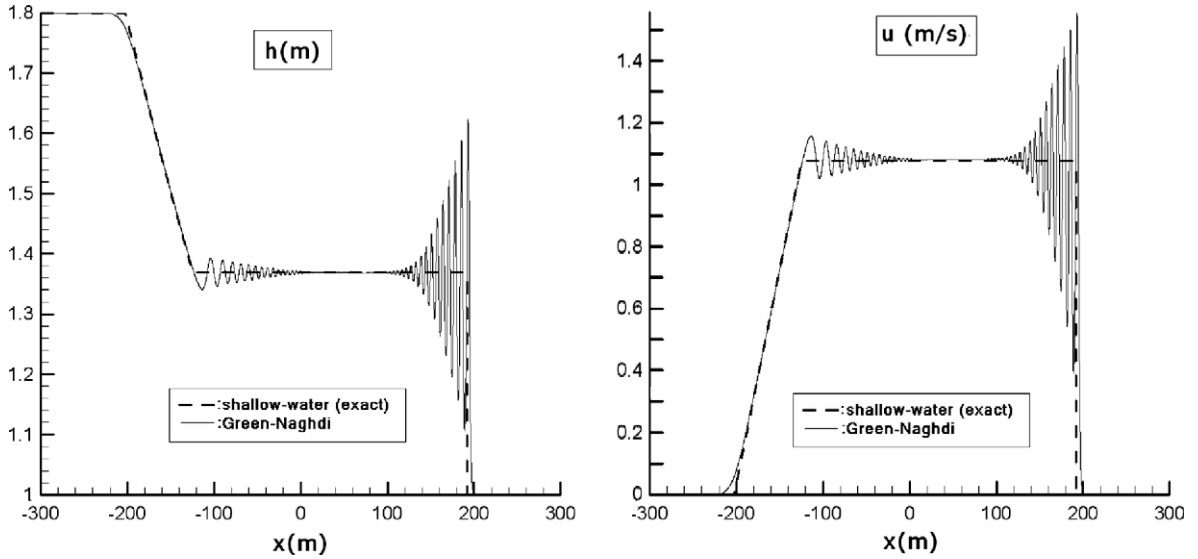

Fig. 5. Numerical solution of the initial value problem (26) for the GN model (1).

The numerical result (lines) with 30,000 cells is presented in Fig. 5 at time $t = 48$ s. The Neumann boundary conditions have been used and the Courant number is 0.8. The resulting numerical solution is compared to the exact "shallow water" solution (dotted lines) at the same time. This last solution corresponds to the resolution of the Riemann problem (26) without dispersive terms. The outcome of such a comparison is obviously to highlight the fact that the plateau values remain unchanged when dispersive effects are taken into account. The presence of these effects only involves localized undular bores clearly visible in Fig. 5.

The Riemann problem for the GN model in this specific configuration has been also numerically solved in [6] by using a finite difference type scheme. In particular, the corresponding solution is highly oscillating at the contact discontinuity. In our case, whatever the number of cells is, the wave form is quite the same and the oscillations are absent at the contact discontinuity as clearly shown in Fig. 5.

6.3. 2D problems

The following initial conditions are considered:

$$h|_{t=0} = \begin{cases} h^-, & \text{if } r < R \\ 0, & \text{if } r > R \end{cases}$$
$$u|_{t=0} = 0$$

This situation corresponds to a spreading of a cylindrical liquid column which was initially at rest, over a rigid wall. The initial values are $h^- = 4.5$ cm, $R = 1$ cm and the square domain is 10 cm $\times$ 10 cm.

The position of the fluid surface is shown in Fig. 6 at different instants. Even if the problem is axisymmetric, this one has been solved numerically by using 2D equations. The Cartesian grid contains 1600 $\times$ 1600 numerical cells. As clearly visible in Fig. 6 the 2D computations preserve the symmetry of the problem. Moreover the treatment of boundary conditions does not lead to artificial oscillations when waves come off the domain as shown in the last graph.

The following test case corresponds to the impact of a liquid cylinder on the rigid surface:

$$h|_{t=0} = \begin{cases} h^-, & \text{if } r < R \\ 0, & \text{if } r > R \end{cases}$$
$$u|_{t=0} = \begin{cases} \frac{\sqrt{2gH}}{2h^-} r, & \text{if } r < R \\ 0, & \text{if } r > R \end{cases}$$

These initial conditions correspond to the case where a cylinder of height h^-, initially at rest at the distance H over the rigid surface, is falling under the gravity and is impacting a horizontal wall.

It is assumed that before impacting the wall the velocity field is uniform inside the liquid column and is equal to $\sqrt{2gH}$. After the impact, the horizontal velocity field is formed compatible with the continuity equation:

$$\frac{\partial h}{\partial t} + \frac{h u_r}{r} + \frac{\partial h u}{\partial r} = 0$$

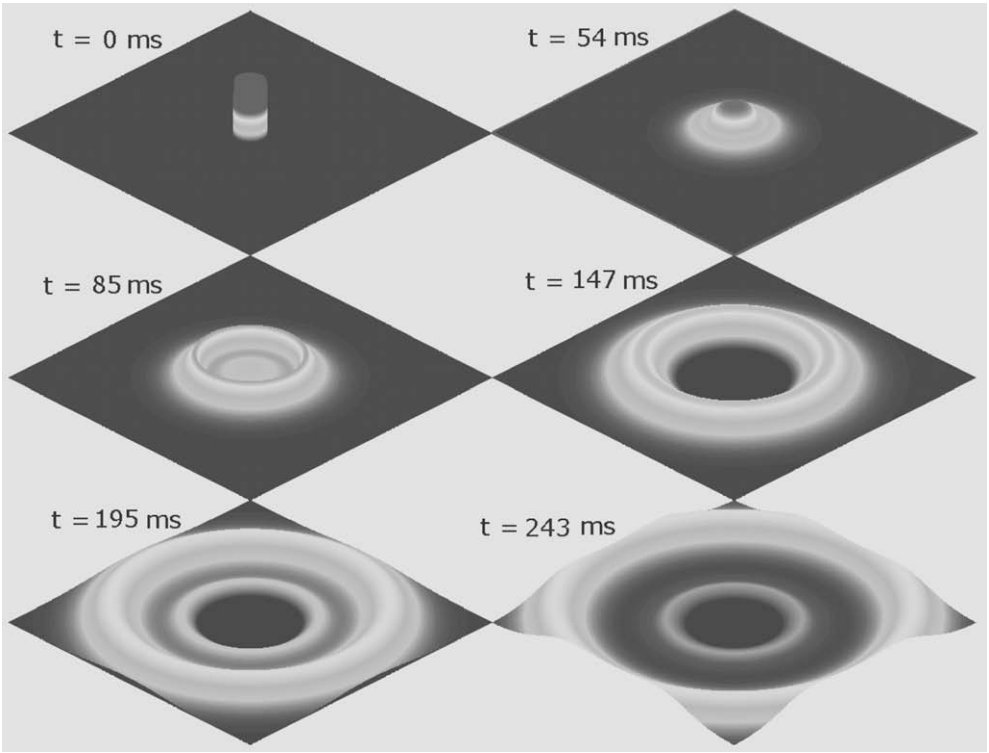

Fig. 6. Numerical solution for the spreading liquid cylinder at different times.

with

$$h_t|_{t=0} = \begin{cases} -\sqrt{2gH}, & \text{if } r < R \\ 0, & \text{if } r > R \end{cases}$$

To compare the solution of the impact problem with real experiments, viscosity terms have been added into the GN system, where the pressure p was replaced by a new pressure $\tilde{p}$:

$$\tilde{p} = p + \gamma \dot{h} = p - \gamma h div \mathbf{u}$$

Here γ is a "viscosity" coefficient. The corresponding energy equation (see (2)) which is compatible with such an "ad hoc" assumption is

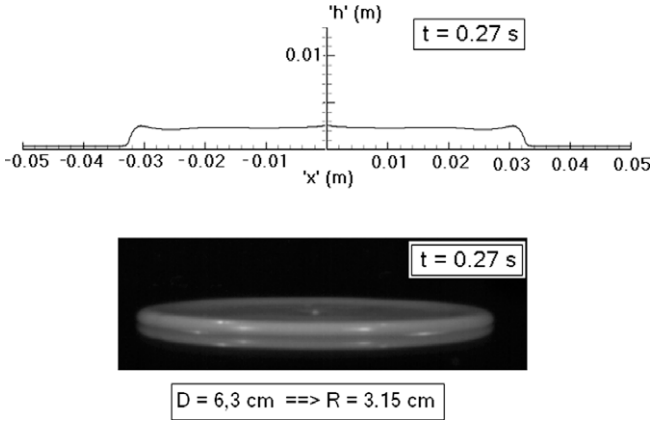

Fig. 7. Comparison between numerical (up) and experimental (down) results concerning the falling cylinder test case at time $t = 0.27$ s. The experimental results were graciously made available to authors by Luu and Forterre.

$$\frac{\partial}{\partial t}\left(\frac{h|\mathbf{u}|^2}{2}+E\right)+div\left(\mathbf{u}\left(\frac{h|\mathbf{u}|^2}{2}+E+p\right)\right)=-(div\mathbf{u})^2\gamma h\leqslant 0.$$

It means that the dissipation terms are correctly introduced. The numerical results with 5000 cells are shown in Fig. 7 at time $t = 0.27$ s. The initial diameter of the falling cylinder is 1.4×10^{-2} m, the initial impact velocity is $\sqrt{2gH}=9\times10^{-2}$ m/s, the initial height of the cylinder is $h^{-}=3.5\times10^{-2}$ m and the "viscosity" coefficient γ (the only empirical constant) is 0.045 m^2/s.

The numerical results are compared with experimental results obtained by Luu and Forterre (2009, private communication) on falling highly viscous clay suspensions. The fluid depth is shown in both cases (numerical and experimental) at time $t = 0.27$ s in Fig. 7. It can be noticed that the structure of the fluid surface is correctly reproduced and the diameters in both cases are in a good agreement.

7. Conclusion

A non-local change of variables has been used for the GN model. A hybrid numerical method based on a Godunov type scheme has been developed to solve that system. Some numerical results have been shown and compared to theoretical and experimental ones. These validations demonstrated the capability of the method to reproduce the wave dynamics appearing in one-dimensional and particular multi-dimensional physical problems. As perspectives, the topography of the bottom as well as the multi-layers (several velocities) must be taken into account in future works with the same numerical strategy.

Acknowledgments

The authors thank referees for important remarks and suggestions.

References

[1] B. Alvarez-Samaniego, D. Lannes, Large time existence for 3D water waves and asymptotics, Invent. Math. 171 (2008) 485–541.
[2] M. Antuono, V. Liapidevskii, M. Brocchini, Dispersive shallow-water equations, Stud. Appl. Math. 122 (2009) 1–28.
[3] G. Bellotti, M. Brocchini, On using Boussinesq-type equations near the shoreline: a note of caution, Ocean Eng. 29 (12) (2002) 1569–1575.
[4] R. Bernetti, E.F. Toro, M. Brocchini, An operator-splitting method for long waves, in: Proceedings of the Long Waves Symposium, 2003, pp. 49–56.
[5] R. Camassa, D.D. Holm, C.D. Levermore, Long-time effects of bottom topography in shallow water, Physica D 98 (1996) 258–286.
[6] G.A. El, R.H.J. Grimshaw, N.F. Smyth, Unsteady undular bores in fully nonlinear shallow-water theory, Phys. Fluids 18 (2006) 027104 (17 pages).
[7] S.L. Gavrilyuk, H. Gouin, A new form of governing equations of fluid arising from Hamilton's principle, Int. J. Eng. Sci. 37 (1999) 1495–1520.
[8] S.L. Gavrilyuk, V.M. Teshukov, Generalized vorticity for bubbly liquid and dispersive shallow water equations, Continuum Mech. Thermodyn. 13 (2001) 365–382.
[9] S.L. Gavrilyuk, V.M. Teshukov, Linear stability of parallel inviscid flows of shallow water and bubbly fluid, Stud. Appl. Math. 113 (2004) 1–29.
[10] A.E. Green, N. Laws, P.M. Naghdi, On the theory of water waves, Proc. R. Soc. Lond. A 338 (1974) 43–55.
[11] A.E. Green, P.M. Naghdi, A derivation of equations for wave propagation in water of variable depth, J. Fluid Mech. 78 (1976) 237–246.
[12] G. Grosso, M. Antuono, E. Toro, The Riemann problem for the dispersive nonlinear shallow water equations, Commun. Comput. Phys. 7 (2010) 64–102.
[13] Y.A. Li, Linear stability of solitary waves of the Green–Naghdi equations, Commun. Pure Appl. Math. 54 (2001) 501–536.
[14] N. Makarenko, A second long-wave approximation in the Cauchy–Poisson problem, Dyn. Contin. Media 77 (1986) 56–72 (in Russian).
[15] J. Miles, R. Salmon, Weakly dispersive nonlinear gravity waves, J. Fluid Mech. 157 (1985) 519–531.
[16] B.T. Nadiga, L.G. Margolin, P.K. Smolarkiewicz, Different approximations of shallow fluid flow over an obstacle, Phys. Fluids 8 (1996) 2066–2077.
[17] R. Salmon, Hamiltonian fluid mechanics, Annu. Rev. Fluid Mech. 20 (1988) 225–256.
[18] R. Salmon, Lectures on Geophysical Fluid Dynamics, Oxford University Press, New York, Oxford, 1998.
[19] C.H. Su, C.S. Gardner, Korteweg–de Vries Equation and Generalizations. III. Derivation of the Korteweg–de Vries Equation and Burgers Equation, J. Math. Phys. 10 (1969) 536–539.
[20] V.M. Teshukov, S.L. Gavrilyuk, Three-dimensional nonlinear dispersive waves on shear flows, Stud. Appl. Math. 116 (2006) 241–255.
[21] E. Toro, Shock-capturing Methods for Free-surface Shallow Flows, Wiley, New York, 2001.
[22] G.B. Whitham, Linear and Nonlinear Waves, John Wiley & Sons, New York, 1974.
[23] J. Yan, C.-W. Shu, A local discontinuous Galerkin method for KdV type equations, SIAM J. Numer. Anal. 40 (2002) 769–791.